THE JOURNAL OF BIOLOGICAL CHEMISTRY VOL. 283, NO. 16, pp. 10813–10821, April 18, 2008

Identification, Characterization, and Structure/Function Analysis of a Corrin Reductase Involved in Adenosylcobalamin Biosynthesis*[S]

Received for publication, December 21, 2007, and in revised form, February 7, 2008 Published, JBC Papers in Press, February 8, 2008, DOI 10.1074/jbc.M710431200

Andrew D. Lawrence[‡], Evelyne Deery[‡], Kirsty J. McLean[§], Andrew W. Munro[§], Richard W. Pickersgill[¶1], Stephen E. J. Rigby[¶], and Martin J. Warren[‡2]

From the [‡]Protein Science Group, Department of Biosciences, University of Kent, Canterbury, Kent CT2 7NJ, [§]Faculty of Life Sciences, Manchester Interdisciplinary Biocentre, University of Manchester, 131 Princess Street, Manchester M1 7DN, and [¶]School of Biological and Chemical Sciences, Queen Mary, University of London, Mile End Road, London E1 4NS, United Kingdom

Vitamin B_{12}, the antipernicious anemia factor, is the cyano derivative of adenosylcobalamin, which is one of nature's most complex coenzymes. Adenosylcobalamin is made along one of two similar yet distinct metabolic pathways, which are referred to as the aerobic and anaerobic routes. The aerobic pathway for cobalamin biosynthesis proceeds via cobalt insertion into a ring-contracted macrocycle, which is closely followed by adenosylation of the cobalt ion. An important prerequisite for adenosylation is the reduction of the centrally chelated metal from Co(II) to a highly nucleophilic Co(I) form. We have cloned a gene, *cobR*, encoding a biosynthetic enzyme with this co(II)rrin reductase activity from *Brucella melitensis*. The protein has been overproduced, and the resulting flavoprotein has been purified, characterized, and crystallized and its structure determined to 1.6 Å resolution. Kinetic and EPR analysis reveals that the enzyme proceeds via a semiquinone form. It is proposed that CobR may interact with the adenosyltransferase to overcome the large thermodynamic barrier required for co(II)rrin reduction.

Cobalamin (vitamin B_{12}) is a coenzyme that is associated with a range of isomerization, methylation, and dehalogenation reactions, utilizing the unique chemistry of the carbon-cobalt bond that is characteristic of this molecule (1). The octahedral geometry of the functional cobalt ion in cobalamin necessitates a structurally complex molecule that consists of a corrin ring, a lower nucleotide loop, and an upper ligand that is either a methyl group in methylcobalamin or an adenosyl group in adenosylcobalamin. The corrin ring is a modified tetrapyrrole and as such bears a structural resemblance to molecules such as heme, chlorophyll, siroheme, and coenzyme F_{430}, reflecting a common synthesis of the tetrapyrrole template as part of a broader branched metabolic pathway (2). However, cobalamin differs from these other modified tetrapyrroles in two important aspects. First, the carbon framework of the corrin molecule has been contracted such that one of the integral carbons of the tetrapyrrole progenitor has been removed to afford a smaller central cavity into which the cobalt ion is bound. Second, cobalamin provides both upper and lower ligands for the cobalt to complement the ligands provided by the nitrogens from the four pyrrole-derived units of the macrocycle.

Central to the role played in catalysis by cobalamin-containing enzymes is the cobalt ion, which forms a unique cobalt-carbon bond with either an upper adenosyl (adenosylcobalamin) or methyl (methylcobalamin) group. It is the physical properties of this bond that mediate the scintillating chemistry associated with B_{12}-dependent transformations (1). There is thus some considerable interest in how this bond is formed in the biosynthesis of vitamin B_{12} (2).

The biosynthesis of cobalamin is a highly complex process, requiring around 30 enzyme-mediated steps for its *de novo* construction (2). The attachment of the upper axial ligand occurs comparatively late in the pathway, after the corrin ring has been synthesized. The attachment of the upper axial ligand requires first reduction of the cobalt ion to Co(I) and second adenosylation, with the transfer of the adenosyl group from ATP (3) (Fig. 1).

There are at least two distinct ways in which nature carries out the reduction of the central cobalt ion within the corrin ring. In organisms that operate the anaerobic pathway for cobalamin biosynthesis, there is no dedicated enzyme for cobalt reduction (4). This conclusion has been reached from a study of the anaerobic biosynthetic B_{12} operons found in many eubacteria in which no specific reductase gene appears to be encoded. Molecular genetic approaches have also failed to find a reductase gene that is dedicated to B_{12} biosynthesis (4). However, other biochemical approaches have shown that the ferredoxin (flavodoxin):$NADP^+$ reductase and flavodoxin A proteins can serve as electron donors for the reduction of co(III)rrinoids to co(I)rrinoids *in vitro* and are therefore likely also to act *in vivo*

* This work was supported by the Biotechnology and Biological Sciences Research Council and Queen Mary, University of London, in the form of a studentship (to A. D. L.). The costs of publication of this article were defrayed in part by the payment of page charges. This article must therefore be hereby marked "*advertisement*" in accordance with 18 U.S.C. Section 1734 solely to indicate this fact.

The atomic coordinates and structure factors (code 3CB0) have been deposited in the Protein Data Bank, Research Collaboratory for Structural Bioinformatics, Rutgers University, New Brunswick, NJ (http://www.rcsb.org/).

[S] The on-line version of this article (available at http://www.jbc.org) contains supplemental text, additional references, and Figs. S1–S6.

[1] To whom correspondence may be addressed: School of Biological and Chemical Sciences, Queen Mary, University of London, Mile End Rd., London E1 4NS, UK. Tel.: 44-20-7882-6360; E-mail: r.w.pickersgill@qmul.ac.uk.

[2] To whom correspondence may be addressed: Dept. of Biosciences, University of Kent, Canterbury, Kent, CT2 7NJ, UK. Tel.: 44-1227-824690; E-mail: m.j.warren@kent.ac.uk.

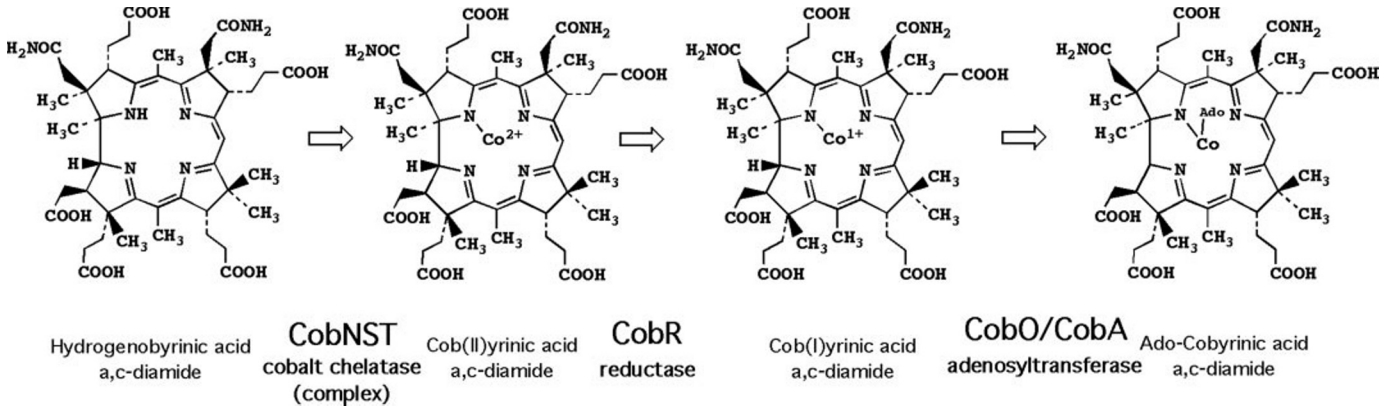

FIGURE 1. **Biosynthesis of vitamin B_{12}, highlighting the transformation of cob(II)yrinic acid *a,c*-diamide into adenonsylcob(III)yrinic acid *a,c*-diamide.** After the insertion of cobalt into the contracted ring system by CobNST, the central cobalt ion of cobyrinic acid *a,c*-diamide is reduced to the Co(I) form by CobR, which acts as a nucleophile for the adenosylation process.

(5). In contrast, along the aerobic pathway, a specific enzyme for the reduction of co(II)rrinoid to co(I)rrinoid has been reported in *Pseudomonas denitrificans*, which acts as soon as the cobalt ion has been inserted into the macrocycle (Fig. 1). In this work, the Rhone Poulenc group isolated an NADH-dependent flavoenzyme exhibiting cob(II)yrinic acid *a,c*-diamide reductase activity and sequenced its N terminus (6). This enzyme of the cobalamin biosynthetic pathway reduced to the Co(I) state all of the Co(II)-corrinoids isolated from this microorganism, indicating a broad substrate specificity. Despite the N-terminal sequencing, the authors were unable to identify the gene encoding this enzyme (7).

In this study we have exploited a bioinformatics approach to identify an orthologous cobalt reductase gene located in a cobalamin biosynthetic operon in the bacterium *Brucella melitensis*. This gene was cloned and expressed, and the encoded protein (CobR) was structurally and functionally analyzed to provide the first systematic characterization of a cobalamin biosynthetic corrinoid reductase.

EXPERIMENTAL PROCEDURES

Molecular Biology—To enable high level expression in *Escherichia coli*, the *cobR* and *cobO* genes were amplified by PCR using genomic DNA from *B. melitensis* as a template. Details of the cloning procedures are given in the supplemental material.

Recombinant Protein Overproduction and Purification—The plasmid bearing the *cobR* gene was transformed into *E. coli* BL12 DE3 pLysS and grown in LB containing 50 mg/liter ampicillin and 30 mg/liter chloramphenicol with aeration at 37 °C. Upon reaching an A_{600} of 1, the culture was induced with isopropyl 1-thio-β-D-galactopyranoside (0.4 mM), and growth was continued overnight at 16 °C. The cells were harvested by centrifugation (20 min, 3,500 × *g*) and resuspended in 10 ml of binding buffer (0.5 M NaCl, 5 mM imidazole, 20 mM Tris-HCl, pH 8.0). Cell lysis was achieved by sonication, and the recombinant protein was purified using immobilized metal affinity chromatography using a column loaded with nickel. Further details are given in the supplemental material.

Activity Assay—Corrin reductase activity was measured as described previously (6).

Electron Paramagnetic Resonance (EPR)—EPR and ENDOR[3] spectra were obtained using a Bruker ELEXSYS E500/580 EPR spectrometer operating at X-band. Temperature control was effected using Oxford Instruments ESR900 and ESR935 cryostats interfaced with an ITC503 temperature controller. Experimental conditions were as given in the figure legends.

Identification of Bound Flavin Cofactor—The purified enzyme was denatured by the addition of ice-cold trichloroacetic acid to a final concentration of 5%. The solution was centrifugation in a bench-top centrifuge to remove precipitate. The supernatant was decanted and neutralized with the addition of 2 M K_2HPO_4, 10 μl of which was injected onto an Ace 5 AQ column (4.6 × 210 mm, 5 μm, Advanced Chromatography Technologies) run on an Agilent 1100 series HPLC equipped with on-line diode array and fluorescence detectors at a flow rate of 1 ml min^{-1}. Flavin cofactors were separated isocratically using 25% methanol in 20 mM KH_2PO_4, pH 7.5, as the eluent. The fluorescence emission at 525 nm was monitored with the excitation wavelength set at 445 nm. Identification of species was based on the comparison of the retention time with that of commercial standards.

Redox Potentiometry—Redox titrations were performed in a Belle Technology glove box under a nitrogen atmosphere as described previously. Further details are given in the supplemental material (8–10).

Crystal Structure of CobR—Purified CobR following removal of the His tag was concentrated to 50 mg ml^{-1}. Bright yellow crystals were obtained using 0.5–1.0 M Li_2SO_4 and 15–20% polyethylene glycol 800 in hanging drop vapor diffusion experiments. CobR crystallized in space group $P2_12_12_1$ with four molecules in the asymmetric unit. Crystals were vitrified by briefly soaking them in mother liquor augmented with 20% (v/v) glycerol before plunging them into liquid nitrogen. Se-Met-labeled CobR was used for *de novo* structure determination using Se-Met SAD-phasing methods. Data collected (720 degrees of data) at the European Synchrotron Radiation Facility (ID29) were processed and scaled using MOSFLM (11) and the CCP4 (12) program suite. After phase generation using autoSHARP

[3] The abbreviations used are: ENDOR, electron nuclear double resonance; HPLC, high pressure liquid chromatography.

TABLE 1
Crystallographic statistics

	High resolution	Selenium peak data
Wavelength (Å)	0.8856	0.9797
Resolution (Å)	1.6	2.2
R_{merge}	6.4 (22.5)[a]	8.8 (20.6)
Mean $I/\sigma(I)$	18.6 (6.8)	35.6 (18.5)
Unique reflections	97,683 (13,967)	38,415 (5482)
% Completeness	99.7 (99.2)	100.0 (100.0)
Multiplicity	3.6 (3.5)	28.9 (29.2)[b]
Mid slope anomalous probability	1.053	1.836
R_{work}	18.3%	
R_{free}	22.3%	
r.m.s. bond lengths (Å)	0.006 (0.021)[c]	
r.m.s. bond angle (°)	1.046 (1.955)	
r.m.s. chiral (Å^3)	0.069 (0.200)	
Ramachandran plot (%)		
Allowed	98.6%[d]	
***B*-factors (Å^2)[e]**		
Protein	11.3	
FMN	15.6	
Waters	35.5	

[a] The overall resolution range is 42.8 to 1.60 Å and in parentheses 1.69 to 1.60 Å for the high resolution data set and 58.5 to 2.2 Å and in parenthesis 2.32 to 2.20 Å for the peak data set.
[b] 720° of data were collected to optimize data quality and facilitate SAD phasing.
[c] For the stereochemical data, the root mean square (r.m.s.) deviations are given, and in parentheses the target (σ) value is shown.
[d] Leu-101 and Ser-140 have clear electron density but fall outside the allowed region of the Ramachandran plot where they account for the disallowed 1.4%.
[e] The mean *B*-factor from the Wilson plot for the high resolution data was 13.8 Å^2.

(13), using four selenium sites, an almost complete model was built using the automatic building procedure ARP/wARP (14). Subsequent cycles of manual model refinement in O (15) and refinement with REFMAC 5 (16) produced the final model at 1.6 Å resolution with one flavin bound per dimer and an R_{work} of 18.3% and an R_{free} of 22.3% (Table 1). FMN was seen bound to CobR, rather than FAD, even when crystals were soaked in fresh FAD immediately prior to data collection.

Substrate Binding—When CobR crystals were soaked in NAD (0.5 mM for 10 min), no NAD was seen in the resulting electron density. However, NAD binding could be modeled using the NAD-bound to flavin reductase (Protein Data Bank code 1RZ0). The flavin reductase-NAD complex and CobR superimpose with a root mean square deviation of 1.8 Å over 1571 equivalenced atoms (17), and superimposition of the two proteins brings the NAD of the flavin reductase into a sterically most plausible position in the CobR cavity.

RESULTS

Identification and Cloning of the Cobalt Reductase—The cobalt reductase was identified from BLAST searches conducted with the published N-terminal sequence (NH_2-MEKTRL) of the *P. denitrificans* corrin reductase enzyme (6). This led to the identification of SMc00514 in *S. meliloti*, which was annotated as being a putative monooxygenase. This sequence was then used in further BLAST searches that produced a list of analogous proteins from a wide range of organisms. From this list a gene encoding an orthologue from *B. melitensis* (BMEI0709) was identified within a cobalamin biosynthetic operon (supplemental Fig. S1). This provided further circumstantial evidence that this protein is likely to be involved in vitamin B_{12} biosynthesis and is a plausible candidate for the corrinoid reductase.

This gene, which has been termed *cobR*, encodes a protein consisting of 173 amino acids with a predicted molecular mass of 18.7 kDa and has primary sequence similarity to a number of flavoproteins, including the smaller reductive component of the 4-hydroxyphenylacetate 3-monooxygenase (either HpaC from *E. coli* or Phe(A2) from *Geobacillus thermoglucosidasius* A7) (supplemental Fig. S1) (18, 19). Some sequence similarity was also observed with PduS (data not shown), a cobalamin reductase that is required for the activation of the diol dehydratase as part of the propanediol utilization metabolosome (20). To investigate the activity of CobR, the gene was amplified by PCR from the genomic DNA of *B. melitensis* and cloned into the vector pET-14b to allow the encoded protein to be produced recombinantly with an N-terminal His tag.

Purification and Characterization of CobR—The cobalt reductase was purified to homogeneity by metal chelate chromatography and gel filtration (supplemental Fig. S2). The isolated protein was highly soluble, and the solution was bright yellow in color. The UV-visible absorbance spectrum is typical of a flavoprotein, with absorption maxima at 380 and 455 nm and characteristic shoulders at 430 and 485 nm (supplemental Fig. S2).

The flavin bound to CobR was identified after the noncovalent cofactor was extracted from the protein by the addition of ice-cold trichloroacetic acid. Following the removal of the precipitate by centrifugation, the supernatant was decanted and neutralized to prevent hydrolysis of FAD. Analysis by reverse phase HPLC revealed that the extracted cofactor exhibited a retention time similar to authentic FAD (supplemental Fig. S3). However, a small quantity of FMN was also present in the extract, which may represent either a limited hydrolysis of the FAD during the extraction procedure or indicate that a small fraction of the purified CobR contains bound FMN. Based on the integral of the peaks, the ratio of FAD to FMN was estimated to be 6:1. Moreover, mass spectral analysis of the flavin, also extracted after acid denaturation of the purified protein, revealed that the major species had a mass consistent with FAD (supplemental Fig. S4).

The observation that FAD is the natural cofactor is further supported by fluorescence titrations of both FMN and FAD with the CobR apoprotein (Fig. 2 and Equation 1).

$$F = F_{end} + F_{\delta}\left(dC_F - \frac{(C_A + K_d + dC_F) - \sqrt{(C_A + K_d + dC_F)^2 - 4C_A dC_F}}{2}\right) \quad \text{(Eq. 1)}$$

where F is the observed emission intensity after each addition; F_{end} is the remaining emission intensity at the end of the titration; F_{δ} is the difference in emission intensity between 1 μM free flavin and 1 μM CobR; C_A is the total protein concentration after each addition (apo + holo); K_d is the dissociation constant of the apoflavin complex in μM units; C_F is the starting concentration of flavin; and d is the dilution factor of this initial concentration (initial volume/total volume) after each addition. The dissociation constants (K_d) for the complexes formed between oxidized FMN and FAD with the apoCobR protein were determined by titrating apoCobR (obtained by dialysis of CobR against guanidine (2 M) and KBr (2 M)) into a known concentration of flavin. By fitting the observed fluorescence as a

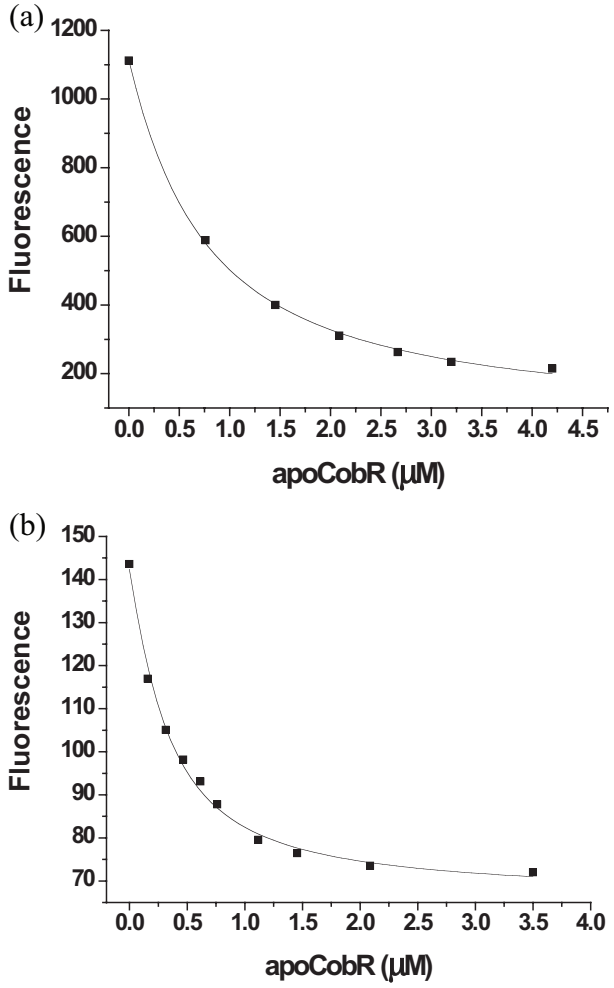

FIGURE 2. **Determination of the dissociation constants for FMN and FAD.** The dissociation constants of the complexes between (*a*) FMN and (*b*) FAD and apoCobR were determined fluorometrically (excitation wavelength 450 nm; emission wavelength 525 nm) by titration of the flavin solution (0.21 μM) with apoCobR, obtained by dialysis of CobR against guanidine (2 M) and KBr (2 M). Dissociation constants were calculated using Origin (OriginLab) by fitting the observed fluorescence as a function of apoCobR concentration in solution as shown in Equation 1.

function of apoCobR concentration, a K_d of 230 ± 27 nM for FAD and 648 ± 46 nM for FMN was determined.

Reduction of CobR—Addition of either NADH or NADPH to a solution of CobR under anaerobic conditions results in bleaching of the cofactor, which is consistent with the reduction of the bound flavin to the $2e^-$ reduced hydroquinone form. Reductive titration against dithionite also revealed that the flavin undergoes an apparent direct reduction to the hydroquinone form, which is inferred from the bleaching of the chromophore and the appearance of an isosbestic point at 340 nm (Fig. 3). This reductive titration was completed over the pH range 4–9, and no significant pH-dependent spectral changes were observed. Equally, no semiquinone formation was observed following rapid mixing of CobR against dithionite by stopped-flow methods. Overall, this indicates rapid disproportionation of the semiquinone and suggests that CobR provides no thermodynamic stabilization for this intermediate.

Redox Potentiometry—In light of the particularly negative redox potential required for the reduction of a corrionoid to the Co(I) state, −610 mV (21), an investigation into the midpoint redox potential for the flavin housed within CobR was undertaken. A solution of CobR in phosphate buffer at pH 7.0 containing 10% (v/v) glycerol was subjected to a reversible spectroelectrochemical titration using dithionite as the reductant and subsequently ferricyanide for the re-oxidation. No hysteresis was observed in oxidative and reductive directions. The data collected at 455 nm (reflecting maximal changes in spectral properties between oxidized and the $2e^-$ reduced enzyme) was fitted to the Nernst equation, which gave an apparent midpoint reduction potential of −207 ± 3 mV for the quinone/hydroquinone transition (Fig. 3).

Corrinoid Reductase Activity—Purified CobR was assayed for Co(III) reductase activities using biosynthetic precursors that included cobyrinic acid, cobyrinic acid *a,c*-diamide, and cobinamide as well as cobalamin (Fig. 4*a*). The specific activity for CobR in the presence of NADH for cobyrinic acid was found to be 4 and 13 μmol/min/mg for cobyrinic acid *a,c*-diamide, 15 μmol/min/mg for cobinamide, and 22 μmol/min/mg for aqua cobalamin.

To determine whether CobR is able to perform the reduction of Co(II) corrinoids to Co(I), a coupled assay in which any Co(I) product formed was converted into the corresponding adenosylated derivative by the adenosyltransferase was used. The conversion of cob(II)alamin into adenosylcobalamin was monitored spectrophotometrically by the corresponding increase in absorbance at 525 nm and quantified using the difference in the molar extinction coefficient of $\Delta\epsilon_{525}$ = 4.8 mM^{-1} cm^{-1} between cob(II)alamin and the product (Fig. 4*b*). Unlike adenosylcobalamin, the β-adenosylated form of cobinamide is yellow, and accordingly, the product of the reaction can be followed by the change in the molar extinction coefficient at 469 nm (Fig. 3*b*), which was estimated to be $\Delta\epsilon_{469}$ = 2.7 mM^{-1} cm^{-1}. The rates of adenosylcobalamin and adenosylcobinamide formation by CobR were found to be at least 3.4 and 9.2 nmol/min/mg, respectively. These values represent minimal rates of activity because the enzyme was not measured under optimal conditions within the confines of the coupled assay. No activity was detected when CobR was omitted from the reaction mixture, and no additional flavin was required for reductase activity. The UV-visible spectra of completed reactions were characteristic of their respective adenosylated derivatives and comparable with previously published data (22). Moreover, after photolysis of the product for 15 min using a 150-watt tungsten lamp at a distance of 20 cm, the optical spectrum returned to that of Co(II) starting material, which is consistent with loss of the adenosyl group. Co(II)rrin reduction activity could also be detected by alkylating the co(I)rrin form by iodoacetic acid in the absence of the adenosyltransferase (data not shown).

CobR Forms a Flavin Semiquinone Radical during Turnover—Evidently, as the enzyme is able to perform the reduction of co(II)rrinoids, CobR must be able to promote the transfer of a single electron from the flavin cofactor to the substrate. This process must proceed through the formation of a flavin semiquinone radical, although reductive methods using dithionite followed by UV-visible spectroscopy have failed to yield this key intermediate (Fig. 3). However, it was possible to identify the flavin semiquinone radical either by employing EPR to

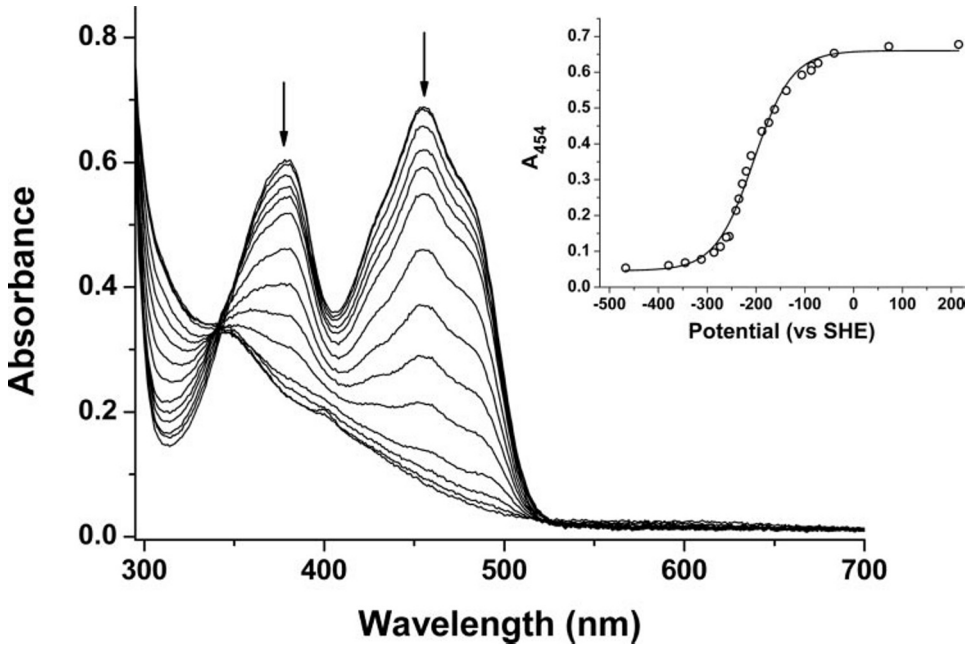

FIGURE 3. **CobR redox titration.** The protein (CobR, 65 μM) was found to be very stable over the time required for the titration allowing full reduction and reoxidation. Spectral changes occurring during the reductive part of the titration are indicated by *arrows*. Fitting data to a Nernst equation results in a midpoint reduction potential of -207 ± 3 mV. *SHE*, standard hydrogen electrode.

monitor single turnover of the reduced enzyme with cob(III)alamin in the forward direction or by reduction of the oxidized protein with cob(I)inamide in the reverse direction. Thus, reduction of the protein with 1 eq of NADH followed by the addition of 1 eq of cob(III)alamin allowed the enzyme to undergo a single turnover. Analysis of the corresponding EPR spectrum revealed that the cob(III)alamin had been reduced to cob(II)alamin and an additional signal was present centered at $g = 2.0032$ consistent with the presence of a semiquinone radical. However, the yield of semiquinone was low, representing only a few percent of the total spin in the sample. The yield of semiquinone could be significantly increased to >50% by rapidly mixing reduced cooled enzyme with cob(III)alamin and quickly freezing the sample. Alternatively, cob(I)inamide could be used as a reductant to reduce the oxidized flavin. The addition of cob(I)inamide (which was generated by reduction of the Co(III) form with sodium borohydride) to a solution of CobR resulted in the oxidation of the cobalt to Co(II) and the formation of the flavin semiquinone.

From such samples it was possible to record the EPR spectrum of the CobR-bound flavin semiquinone radical (Fig. 5*a*). Despite it not being possible to observe any resolved hyperfine structure from flavoprotein radicals, because of the multiplicity and anisotropies of the hyperfine interactions, it was possible to obtain some structural information from the line width of the EPR signal. An anionic, or red, semiquinone will typically exhibit a line width of ~15 G, whereas a neutral, or blue, semiquinone is identified from a broader line width of around 19 G (23). With the line width of the CobR spectrum being 20.3 G, the signal has been assigned to that of a blue flavin semiquinone.

The Davies ENDOR spectrum of the flavosemiquinone (Fig. 5, *b* and *c*) shows several features previously assigned in ENDOR spectra of neutral flavosemiquinones (24–26). The most prominent features can be assigned to the $A_\perp$ (**b**) and $A_\parallel$ (**d**) components of the hyperfine coupling to the 8-methyl protons of the flavosemiquinone. Also evident are features, **a**, previously assigned to a component of the 6H hyperfine coupling. The use of a first derivative presentation allows for the observation of the lines **c** and **e**. These have previously been assigned as the $A_\perp$ and $A_\parallel$ components, respectively, of a hyperfine coupling to one of the C-1′-ribityl protons attached to the flavosemiquinone at N-10 (24). There are many more features of the ENDOR spectrum lying between 12.5 and 17.5 MHz that could arise from either weak hyperfine coupling to flavosemiquinone protons or hyperfine coupling to protein protons. Further studies employing orientation selected ENDOR, H_2O-D_2O exchange, and specific deuteration of CobR will allow for the assignment of these lines.

The hyperfine coupling to the 8-methyl protons is greater than that reported for many other protein-bound neutral flavosemiquinones or for the neutral flavosemiquinone *in vitro* being $A_\perp = 8.0$ Mhz and $A_\parallel = 9.6$ MHz. The isotropic hyperfine coupling of the 8-methyl protons, $\frac{1}{3}(2A_\perp + A_\parallel)$, is related to the unpaired electron spin density, ρ, at C-8 via the McConnell relation $A_{iso} = Q\rho_{C\text{-}8}$ (27), where the constant $Q = 81$. Thus the $A_{iso} = 8.5$ MHz, and $\rho_{C\text{-}8}$ is 0.104. This is somewhat higher than previously reported for many protein-bound flavosemiquinones and suggests that more of the unpaired electron spin density of the radical state is located at C-8 than in other flavoproteins. This may reflect the role of the dimethylbenzene part of the flavin, and the C-8 methyl group in particular, in electron transfer to Co(II)-corrinoids.

Crystal Structure—Purified CobR was found to crystallize readily (Fig. S2). The crystal structure of CobR was solved *de novo* using single wavelength anomalous dispersion data and refined at 1.6 Å resolution to give a structure with good stereochemistry and with a R_{work} and R_{free} of 18.3 and 22.3%, respectively (see "Experimental Procedures"). Two CobR homodimers (four polypeptide chains) were present in the asymmetric unit, and within each homodimer the subunits are in close contact related by a pseudo 2-fold rotation axis. There was clear electron density for residues 8–173, 11–173, 12–173, and 13–173 for chains A, B, C, and D, respectively; the N-terminal part of the polypeptide chain is presumably rather flexible. The intimacy of the subunits in the crystal combined with solution data, which show CobR is a dimer, strongly suggest the dimer observed in the crystal is biologically authentic (Fig. 6*a*). More surprisingly was the observation that the flavin was FMN and not FAD, the preferred physiological cofactor. Moreover,

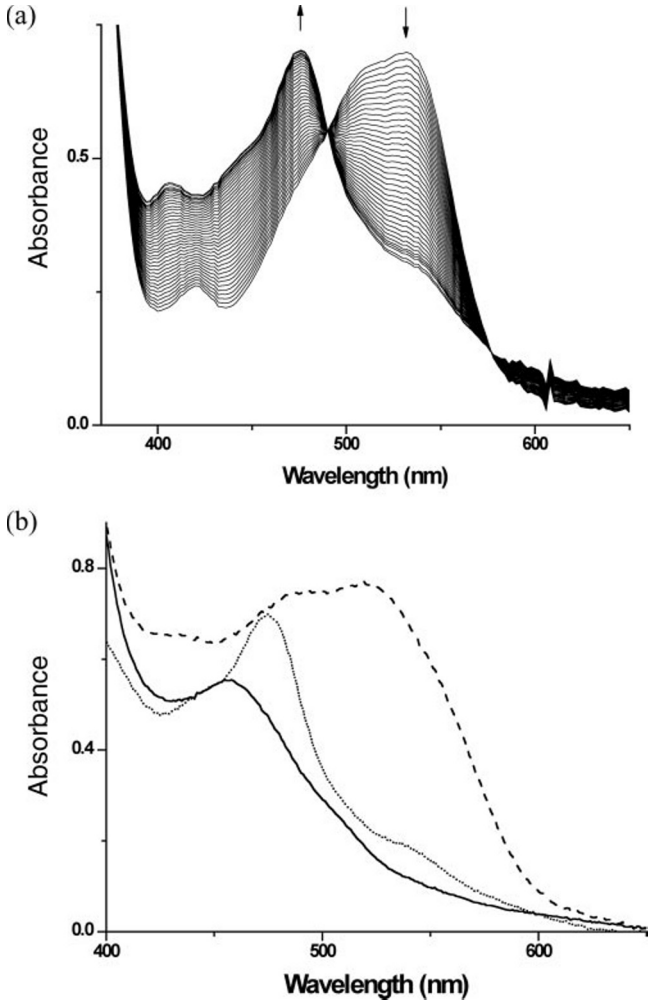

FIGURE 4. **Spectra obtained during the transformation of co(III)rrin to co(II)rrin and co(II)rrin to co(I)rrin.** *a,* transformation of cob(III)alamin into cob(II)alamin. Diode array UV-visible spectra showing the CobR-dependent reduction of 50 μM cob(III)alamin to cob(II)alamin. Reaction mixture contained 50 μM cob(III)alamin, 0.5 mM NADH, and 0.5 μg of CobR. *b,* transformation of cob(II)alamin and cob(II)inamide into their adenosylated derivatives. The spectrum of the co(II)rrin starting material is shown as a *dotted line* (both cob(II)alamin and cob(II)inamide give the same spectrum). Incubation of cob(II)alamin with CobR, ATP, NADH, and the adenosyltransferase CobO generated the *dashed line* spectrum (adenosylcobalamin), whereas incubation with cob(II)inamide produced the *solid line* spectrum (adenosylcobinamide).

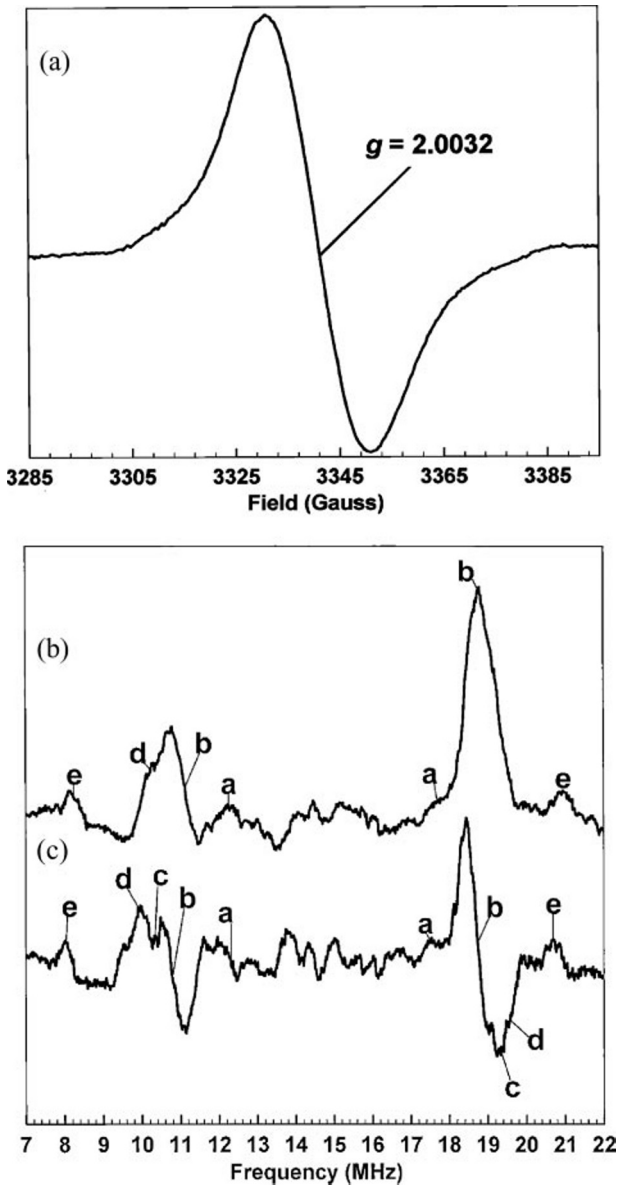

FIGURE 5. **EPR and ENDOR spectra of the CobR-bound flavin semiquinone.** *a,* X-band EPR spectrum of flavosemiquinone form of CobR formed by the rapid mixing of NADH-reduced CobR with co(III)rrin, followed by rapid freezing in liquid nitrogen. Experimental parameters are as follows: microwave power 5 microwatts, modulation frequency 100 kHz, modulation amplitude 1.2 G, temperature 20 K. *b,* X-band Davies pulsed ENDOR spectrum of the CobR flavosemiquinone formed as in *a*. *c,* first derivative presentation of *b*. Temperature for ENDOR spectra was 120 K, resulting spectrum is the sum of 120 scans.

only one of the subunits in the dimer binds the flavin FMN (Fig. 6*b*) despite the subunits being closely similar (root mean square deviation is 0.375 Å for 1114 equivalent atoms). The major difference between the two subunits is in the position of Arg-98 and this might influence the binding of FMN to the CobR subunit (supplemental Fig. S5). The Dali Server (28) reveals that the closest known structure to CobR is that of the *G. thermoglucosidasius* flavin reductase (Protein Data Bank code 1RZ0) with a root mean square deviation 1.6 Å over 146 equivalent residues (29).

The core of the CobR subunit is a six-stranded anti-parallel β-barrel formed from β-strands (β1, β2, β4, β5, β6, and β7) and capped by an α-helix (α2). Two additional α-helices (α3 and α4) flank the central β-barrel and the remaining α-helix (α1) embraces the other subunit stabilizing the dimer (Fig. 6*a*). The subunit adopts a FMN-binding split barrel fold (Greek key architecture), related to the ferredoxin reductase-like FAD-binding domains.

Description of the Flavin-binding Site—The FMN molecule present in the structure is bound in a groove in the surface of the enzyme between α2 and α3, along the edge of β2. The *si* face of the isoalloxazine ring is buried, but the *re* face is orientated into the large solvent-filled cavity formed between the two subunits. The flavin reductase binds FAD, and there is a distinct adenosine-binding site. In CobR, however, there is no equivalent adenine-binding pocket observed in the structure, and the corresponding region of the protein is occupied by α4 (Fig. 6*c*). Solution studies show the presence of adenosine contributes to binding affinity, and this may be via entropic effects (release of water from the adenosine surface) rather than enthalpic inter-

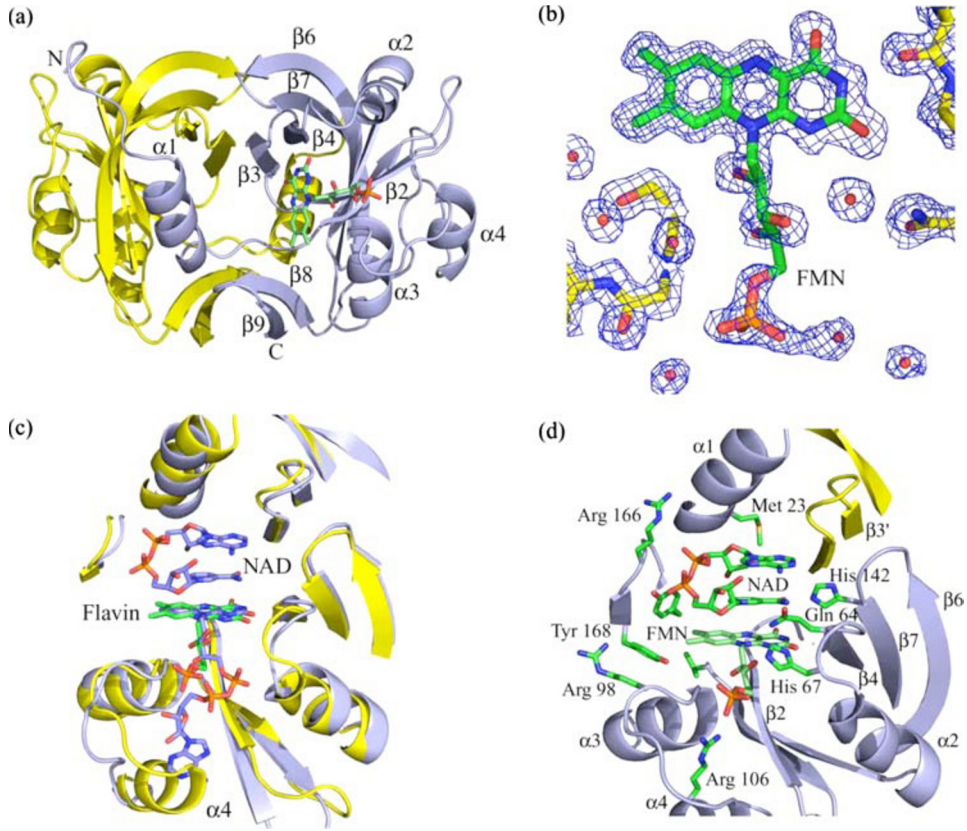

FIGURE 6. **Crystal structure of CobR.** *a,* schematic representation of the homodimer architecture of CobR with FMN shown in *stick* representation. The *si* face of the FMN is presented to the large central cavity. *b,* σ_A weighted $2F_{obs} - F_{calc}$ Fourier synthesis showing the quality of the electron density corresponding to the isoalloxazine ring of the bound FMN; the electron density is contoured at 1σ (*blue mesh*). *c,* schematic representation showing the superimposition of flavin reductase (Phe(A2)) and CobR, which brings the isoalloxazine rings of the flavins shown in *stick* representation into close structural alignment. The position of α-helix α4 of CobR precludes the binding of adenosine at the corresponding position in CobR, and there is no adjacent binding pocket that can accommodate the adenosine. The NAD bound by flavin reductase can be readily accommodated in CobR. *d,* more detailed view of FMN and proposed NAD binding in CobR showing some key interactions with FMN and NAD. The measured distance between the modeled NAD (nicotinamide) C-5 and the experimentally observed isoalloxazine ring N-5 of 3.2 Å is consistent with hydride transfer from C-5 of NADH to N-5 of FMN. Produced using PyMol (17).

actions. The residues involved in binding the flavin originate from a single subunit, and there is no indication of interactions across the dimer interface. The 2,4-pyrimidinedione moiety of the flavin forms an extensive network of hydrogen bonds with main chain atoms from residues Ala-48, Cys-62, and Gln-64 along with a water molecule. The phosphate moiety also forms a number of hydrogen bonds to the main chain atoms of residues Thr-45 and Phe-95 together with a water molecule and the side chain of Arg-106, which is coordinated to the phosphate group itself. The dimethylbenzene moiety resides in a hydrophobic pocket formed mostly from the side chains of residues Val-30, Tyr-163, and Tyr-168 (Fig. 6*d*). Significantly, in the current conformation, there is no suitable hydrogen bonding partner in range of nitrogen N-5 of the isoalloxazine ring. A strong hydrogen bond between N-5 and the protein is known to provide a degree of thermodynamic stabilization for the semiquinone radical (30). However, this may be a consequence of the oxidation state of the flavin in the structure. It is well known that small changes in the protein structure around the flavin occur upon reduction, and these changes can influence the redox potential of the flavin (31). Thus, it is feasible that in the semiquinone structure, the side chain of Thr-47 (currently 3.7 Å away) or a water molecule may be brought within hydrogen bonding range. However, it should also be noted that the flavin semiquinone occurs only fleetingly and is barely detectable unless the enzyme is frozen rapidly during turnover.

The residue whose position differs the most between the two subunits in the dimer is Arg-98, where the side chain adopts two conformations. In the subunit with the bound flavin (subunit A), the side chain is in an "out" conformation and forms a salt bridge with Asp-93 of subunit C from the other dimer in the asymmetric unit. In the monomer lacking a bound cofactor, Arg-98 adopts the "in" conformation where it lies parallel to the ribityl-binding site (supplemental Fig. S5). The effect of Arg-98 appears to be minor, but its contribution to protein electrostatics might influence flavin affinity.

Description of the NAD-binding Site—Structurally aligning the *G. thermoglucosidasius* flavin reductase (29) and CobR brings the flavin isoalloxazine rings into close structural alignment and the NAD into the solvent-filled cavity of CobR. The NAD can be comfortably accommodated within the cavity present in CobR (Fig. 6*c*). Arg-20 could readily move to hydrogen bond the NAD phosphates and His-142 and Ser-51 (from the other subunit) are ideally positioned to hydrogen bond the adenosine N-3 and nicotinamide amide N-7, respectively. Additional hydrogen bonds could be made to stabilize this unusual bent NAD conformation. Significantly, for hydride transfer to the flavin from NADH, the nicotinamide C-4 and FMN N-5 are separated by only 3.2 Å in this modeled ternary complex.

DISCUSSION

We have identified a potential corrin reductase that is part of the cobalamin biosynthetic pathway in *B. melitensis*. Several lines of evidence make the case compelling. First, the enzyme is related in both sequence and physical characteristics to the enzyme previously reported by the Rhone Poulenc group (6). Moreover, there is sequence similarity between CobR and a cobalamin reductase (PduS) that has recently been described as part of the propanediol utilization machinery (20). Second, CobR exhibits both co(III)rrinoid and co(II)rrinoid reductase activities and displays a wide substrate specificity, from cobyrinic acid to cobalamin. A comparison of the reduction rates

indicates an apparent preference for amidated side chains on the modified tetrapyrrole substrate, which is consistent with cobyrinic acid *a,c*-diamide being the true pathway intermediate as reported previously (6).

CobR Is a Flavoprotein—The biochemical characterization of the protein revealed that it has a preference for FAD over FMN, and the as-isolated protein contained more bound FAD than FMN. However, the crystal structure of CobR revealed that only FMN was bound. The presence of FMN in the crystallized CobR could be due to the preferential crystallization of the FMN-containing form of the enzyme, or perhaps due to hydrolysis of bound FAD under the relatively high pH crystallization conditions.

CobR Is Reduced by NADH—The reduced flavin on CobR then facilitates the single electron reduction of the metal center in the corrin substrate. This process generates a flavin semiquinone that disproportionates rapidly. The lack of any semiquinone upon equilibrium reduction of CobR by dithionite is further evidence that this intermediate is not stabilized within the enzyme. During the catalytic cycle of CobR, the semiquinone can either be used to promote a second round of corrin reduction or it may be disproportionate within the protein dimer with the flavin in the second active site, or with a flavin in a separate dimer.

The enzyme has an overall similar topology to another characterized flavoprotein, the flavin reductase component (HpaC or PheA2) of the 4-hydroxyphenylacetate 3-hydroxylase (29, 32, 33). The bound flavin in HpaC is reduced by NADH, and the reduced enzyme is then able to reduce free flavin, which diffuses to the hydroxylase component (34). Crystal structures of HpaC with NAD^+ have been solved revealing that the NAD^+ is bound in a bent configuration (29, 32, 33). Given the active site topology an assumption can be made that NADH is also likely to bind in this conformation within CobR, and it is therefore possible to compose a symphony of events that would allow corrin reduction to take place within CobR. The exquisite positioning of appropriate hydrogen bonding groups in the cavity to the *si* face of the flavin ring in CobR reveals that NADH will bind to CobR in the same bent conformation as seen in the flavin reductase (29, 32, 33). This would facilitate hydride transfer from the nicotinamide ring of NADH to the N-5 of the flavin. Upon the release of the spent NAD^+ and its diffusion from the active site, the corrin ring (either Co(III) or Co(II)) then occupies the vacant cavity. Molecular modeling suggests that the corrin is able to bind to CobR in the active site with the cobalt ion in closer proximity to the dimethylbenzene end of the isoalloxazine ring of the flavin (data not shown). Such a binding configuration favors single electron transfer to the corrin and is supported by the high unpaired electron spin density at C-8 observed in ENDOR spectra of the semiquinone state. EPR studies using low spin Co(II) corrinoids supports the idea that the various corrin substrates bind directly to the enzyme (data not shown).

To catalyze the reduction of co(II)rrin to co(I)rrin, the enzyme has to overcome a significant energy barrier. The midpoint potential for corrin reduction is predicted to be around −500 mV for cobinamide and −610 mV for cobalamin (21), which is in stark contrast to the significantly higher midpoint potential for the co(III)rrin to co(II)rrin reduction (35). For the one-electron reduction process involved in corrin reduction, the relevant parameters that need to be measured include the flavin hydroquinone/semiquinone and semiquinone/FAD couples. However, it was not possible to measure these values because of the instability of the flavin semiquinone form within CobR. Nonetheless, the midpoint redox potential of the two-electron reduction of the flavin in CobR was found to be -207 ± 3 mV. Thus CobR is much more efficient at reducing the latter, and this is reflected in the relative rates of reduction of the co(III)rrin and co(II)rrin substrates.

The unfavorable reduction of the co(II)rin intermediate undoubtedly reflects the very negative redox potential of the process. One way to overcome this thermodynamically unfavorable reaction would be to couple it to a process that is much more thermodynamically favorable. Hence, co(II)rrin reduction could be coupled with the adenosylation of the corrin. In support of this idea, we have shown that CobR appears to interact with the *B. melitensis* CobO (the cob(I)yrinic acid *a,c*-diamide adenosyltransferase (36, 37), which is sometimes referred to as CobA or BtuR (38, 39)) through the increase in fluorescence polarization observed on the titration of CobO into a solution of CobR (supplemental Fig. S6). Others have suggested that corrin reduction may take place on the adenosyltransferase itself, as co(II)rrinoids appear to bind in a unique four-coordinate manner on the enzyme to assist in the reduction process (40). However, as co(II)rrin reduction can take place in the absence of the adenosyltransferase, and as the corrin can bind to CobR, there may be fundamental differences between the reduction processes that take place during biosynthesis and salvage.

Acknowledgment—The B. melitensis genomic DNA was a generous gift from Professeur Jean-Jacques Letesson, Facultes Universitaires Notre-Dame de la Paix.

REFERENCES

1. Banerjee, R., and Ragsdale, S. W. (2003) *Annu. Rev. Biochem.* **72,** 209–247
2. Warren, M. J., Raux, E., Schubert, H. L., and Escalante-Semerena, J. C. (2002) *Nat. Prod. Rep.* **19,** 390–412
3. Debussche, L., Thibaut, D., Cameron, B., Crouzet, J., and Blanche, F. (1993) *J. Bacteriol.* **175,** 7430–7440
4. Fonseca, M. V., and Escalante-Semerena, J. C. (2000) *J. Bacteriol.* **182,** 4304–4309
5. Fonseca, M. V., and Escalante-Semerena, J. C. (2001) *J. Biol. Chem.* **276,** 32101–32108
6. Blanche, F., Maton, L., Debussche, L., and Thibaut, D. (1992) *J. Bacteriol.* **174,** 7452–7454
7. Blanche, F., Cameron, B., Crouzet, J., Debussche, L., Thibaut, D., Vuilhorgne, M., Leeper, F. J., and Battersby, A. R. (1995) *Angew. Chem. Int. Ed. Engl.* **34,** 383–411
8. Dutton, P. L. (1978) *Methods Enzymol.* **54,** 411–435
9. Munro, A. W., Noble, M. A., Robledo, L., Daff, S. N., and Chapman, S. K. (2001) *Biochemistry* **40,** 1956–1963
10. Ost, T. W., Miles, C. S., Munro, A. W., Murdoch, J., Reid, G. A., and Chapman, S. K. (2001) *Biochemistry* **40,** 13421–13429
11. Leslie, A. G. W. (1992) *Joint CCP4 + ESF-EAMCB Newsletter on Protein Crystallography*, No. 26
12. Collaborative Computational Project No. 4 (1994) *Acta Crystallogr. Sect. D. Biol. Crystallogr.* **50,** 760–767
13. de La Fortelle, E., Bricogne, G., and Charles W. Carter, Jr. (1997) *Methods*

Enzymol. **276,** 472–494
14. Lamzin, V. S., and Wilson, K. S. (1997) *Methods Enzymol.* **277,** 269–305
15. Jones, T. A., Zou, J. T., Cowan, S. W., and Kjeldgaard, M. (1991) *Acta Crystallogr. Sect. A.* **47,** 110–119
16. Murshudov, G. N., Vagin, A. A., and Dodson, E. J. (1997) *Acta Crystallogr. Sect. D. Biol. Crystallogr.* **53,** 240–255
17. DeLano, W. L. (2002) *The PyMOL Molecular Graphics System,* DeLano Scientific LLC, San Carlos, CA
18. Arunachalam, U., Massey, V., and Vaidyanathan, C. S. (1992) *J. Biol. Chem.* **267,** 25848–25855
19. Prieto, M. A., and Garcia, J. L. (1994) *J. Biol. Chem.* **269,** 22823–22829
20. Sampson, E. M., Johnson, C. L. V., and Bobik, T. A. (2005) *Microbiology* **151,** 1169–1177
21. Lexa, D., and Saveant, J. M. (1983) *Acc. Chem. Res.* **16,** 235–243
22. Thomas, M. G., and Escalante-Semerena, J. C. (2000) *J. Bacteriol.* **182,** 4227–4233
23. Palmer, G., Muller, F., and Massey, V. (1971) in *Flavins and Flavoproteins* (Kamin, H., ed) pp. 123–140, University Park Press, Baltimore, MD
24. Kay, C. W. M., Feicht, R., Schulz, K., Sadewater, P., Sancar, A., Bacher, A., Mobius, K., Richter, G., and Weber, S. (1999) *Biochemistry* **38,** 16740–16748
25. Kurreck, H., Bock, M., Bretz, N., Elsner, M., Kraus, H., Lubitz, W., Muller, F., Geissler, J., and Kroneck, P. M. H. (1984) *J. Am. Chem. Soc.* **106,** 737–746
26. Weilbacher, E., Helle, N., Elsner, M., Kurreck, H., Muller, F., and Allendoerfer, R. D. (1988) *Magn. Reson. Chem.* **26,** 64–72
27. McConnell, H. M. (1956) *J. Chem. Phys.* **24,** 764–766
28. Holm, L., and Sander, C. (1993) *J. Mol. Biol.* **233,** 123–138
29. van den Heuvel, R. H., Westphal, A. H., Heck, A. J., Walsh, M. A., Rovida, S., van Berkel, W. J., and Mattevi, A. (2004) *J. Biol. Chem.* **279,** 12860–12867
30. Muller, F., Hemmerich, P., Ehrenberg, A., Palmer, G., and Massey, V. (1970) *Eur. J. Biochem.* **14,** 185–196
31. Ludwig, M. L., Pattridge, K. A., Metzger, A. L., Dixon, M. M., Eren, M., Feng, Y., and Swenson, R. P. (1997) *Biochemistry* **36,** 1259–1280
32. Kim, S. H., Miyatake, H., Hisano, T., Ohtani, N., and Miki, K. (2003) *Acta Crystallogr. Sect. D. Biol. Crystallogr.* **59,** 2275–2278
33. Okai, M., Kudo, N., Lee, W. C., Kamo, M., Nagata, K., and Tanokura, M. (2006) *Biochemistry* **45,** 5103–5110
34. Galan, B., Diaz, E., Prieto, M. A., and Garcia, J. L. (2000) *J. Bacteriol.* **182,** 627–636
35. Pratt, J. M. (1999) in *Chemistry and Biochemistry of B12* (Banerjee, R., ed) pp. 113–164, John Wiley & Sons, Inc, New York
36. Crouzet, J., Levy-Schil, S., Cameron, B., Cauchois, L., Rigault, S., Rouyez, M. C., Blanche, F., Debussche, L., and Thibaut, D. (1991) *J. Bacteriol.* **173,** 6074–6087
37. Debussche, L., Couder, M., Thibaut, D., Cameron, B., Crouzet, J., and Blanche, F. (1991) *J. Bacteriol.* **173,** 6300–6302
38. Bauer, C. B., Fonseca, M. V., Holden, H. M., Thoden, J. B., Thompson, T. B., Escalante-Semerena, J. C., and Rayment, I. (2001) *Biochemistry* **40,** 361–374
39. Escalante-Semerena, J. C., Suh, S. J., and Roth, J. R. (1990) *J. Bacteriol.* **172,** 273–280
40. Stich, T. A., Buan, N. R., Escalante-Semerena, J. C., and Brunold, T. C. (2005) *J. Am. Chem. Soc.* **127,** 8710–8719